Biogas-fed Solid Oxide Fuel Cell (SOFC) coupled to tri-reforming process: modeling and simulation.

Flavio Manenti[a,*], Paolo Vallevi[a], Andres Ricardo Leon Garzon[a], Renato Pelosato[a], Giovanni Dotelli[a], Antonio Vita[b], Massimiliano Lo Faro[b], Gaetano Maggio[b], Lidia Pino[b], Antonino S. Aricò[b]

[a] Politecnico di Milano, Dipartimento di Chimica, Materiali e Ingegneria Chimica "Giulio Natta", Piazza Leonardo da Vinci 32, 20133 Milano, Italy.

[b] CNR-ITAE, Istituto di Tecnologie Avanzate per l'Energia "Nicola Giordano", Via Salita S. Lucia sopra Contesse 5, 98126 Messina, Italy.

Prepared for the Special Issue of the International Journal of Hydrogen Energy

[*] Corresponding Author:

Email: xxx; Phone: +39nnn; Fax: +39nnn

Abstract

The present work deals with the modeling, simulation and model validation of a biogas-fed tri-reformer followed by a solid oxide fuel cell (SOFC) for power generation, and a furnace for pre-heating of the stream entering the system. The PRO/II® software, for the simulation of the tri-reforming process, and ad-hoc models for the SOFC and the furnace, were used in order to predict results on a micro-scale plant. Experimental results were outlined in a previous work [1]. The overall system model was validated with the experimental data carried out in laboratory scale. The performance achieved on the simulated micro-scale plant was low, due to the experimental conditions modeled; nonetheless, the inherent flexibility of the model allows its application for the assessment of larger systems operating in real conditions.

1. Introduction

Due to several economic, environmental and societal factors, dependence on fossil fuels for energy production and transportation has proven to be unsustainable in the long term [2]. As a result, great attention has been paid to the utilization of renewable energy sources and to the efficiency improvements.

Hydrogen is one of the most promising renewable energy carrier, as it is versatile, clean and ubiquitous up to the point that the term “hydrogen economy” has been coined to indicate a post-fossil-fuel world [3]. Even though there are still several technical difficulties to overcome in the production, transportation and storage of hydrogen to make it completely sustainable, one of the most serious drawbacks is the selection of a proper source to procure it. Hydrogen is a secondary energy carrier: it is not found in free-state in nature, and must be obtained from other primary fuels. Traditionally, it is produced from fossil sources through steam reforming (SR) or partial oxidation (POX) of hydrocarbons (usually, methane), or coal gasification. It can also be obtained from non-fossil sources through the electrolysis of water, biomass gasification and reforming of biogas, [4-6], which is one of the most widespread renewable fuels. Indeed, biogas can be obtained from various biomasses and processes such as degradation of urban and industrial waste, landfills, co-digestion of zootechnical effluents, agricultural wastes and energy crops [7]. It consists of a mixture of methane (40-70% vol.) and carbon dioxide (30-60% vol.) and traces of other gases (1-5% vol.), like hydrogen (0-1% vol.) and hydrogen sulphide (0-3% vol.). Even though biogas is nowadays mostly used to produce heat and electricity through power turbines and internal combustion engines, sometimes employing biogas in such systems could result in low electrical conversions, high levels of noise, maintenance problems and pollutant emissions [1]. In this context, hydrogen can play an important role that can fill the gap for employing biomass derived fuels in more efficient power generation systems such as fuel cells (FCs), as recently a combination of such systems with reforming processes has been proposed [8, 9].

A fuel cell is an electrochemical device that directly converts chemical energy from a fuel into electric power and heat. Fuel cells are clean, efficient and silent; they can be applied in large-scale systems for power distribution; in portable power supply systems for microelectronic devices; or as auxiliary power units in vehicles [10]. Such devices work by an electrochemical oxidation-reduction (redox) reaction which takes place at the cathode and at the anode of the cell. They can use a variety of fuels and oxidants, but nowadays the interest is centred on hydrogen as fuel, and air as oxidant [11]. In particular, solid oxide fuel cells (SOFCs) are considered the simplest fuel cell concept available on the market, as there are only two phases involved in the system (gas and solid); they operate in temperatures ranging from 600°C to 1000°C and thus are characterized by high reaction rates. The electrolyte is an ion-conducting ceramic typically composed of yttria-stabilised zirconia (YSZ) or Gadolinium-doped Ceria (GDC), that at high temperature become good oxygen ion conductors. On the other hand, the anode is typically a nickel-YSZ cermet, and the cathode is based on perovskites, such as Sr-doped $LaMnO_3$ and $La_{1-x}Sr_xFe_{1-y}Co_yO_3$. Solid oxide fuel cells allow the integration of all the fuel processing stages from purification to conversion (i.e. reforming) and additionally the cogeneration at high temperatures [8]. The purification step is necessary to remove poisonous agents such as H_2S, NH_3, halides, siloxanes and other species that could affect the performance of the reforming catalyst or the nickel anode [12].

Among the possible biogas reforming processes, Dry Reforming (DR) seems an appropriate option since the major constituents of the biogas are CH_4 and CO_2. The major issue of DR is the requirement of high temperatures to reach high conversion levels, these severe operating conditions result in deactivation of the catalyst caused by sintering of the metallic phase and support [13] and by coke deposition [14]. The Steam Reforming (SR) gives more hydrogen yields compared with DR reaction [15], but, as DR process, it requires an external heat source to supply the endothermic reactions and to preheat the reforming agent (steam), this, reduces the overall efficiency of the fuel processor and of the global system (Processor-SOFC) [16]. As DR, the SR process ~~are~~ is characterized by several operational issues related with the degradation of the catalyst by coke deposition and sintering of the metallic phase [1].

Also the Catalytic Partial Oxidation (CPOX) process have been proposed to produce hydrogen/syngas from biogas, due to its exothermicity, CPOX is considered most promising, in terms of energy saving, compared to the SR and DR processes [17,18]. However, CPOX can present several problems, including risk of explosion and hotspot formation, with consequent catalyst deactivation, which results in loss of activity [19,20].

A new catalytic process that may addresses these issues is called tri-reforming: it simultaneously combines all the above processes in a single step [21]. In such a process, the carbon deposition on the catalyst is avoided by the presence of water and oxygen, and the energy requirements are reduced, due to the combination of the two endothermic processes (i.e. dry and steam reforming) with an exothermic one (i.e. partial oxidation). An important benefit of the tri-reforming process is the inherent flexibility of the system itself; in fact, by simply modifying the process variables such as temperature, O_2/CH_4 and H_2O/CH_4 ratios, it is possible to achieve an auto-thermal operation [22]. In the same way, such modifications allow to modulate the syngas final composition. Therefore, it can be used for the production of chemicals (such as methanol or dimethyl ether) [23], synthetic ultraclean fuels (through the Fischer-Tropsch synthesis, [24]) or the generation of electric power (through a fuel cell, such as in the case of the present work). As explained earlier, the tri-reforming process allows a safer operation for the catalyst, as the presence of both oxygen and water greatly reduces carbon deposition. Additionally, the milder thermal operation allows the safeguard of the catalyst from sintering. Finally, the tri-reforming process can be carried out by feeding gases having various compositions; thus, it can use methane and carbon dioxide from a large number of sources [1, 21].

The catalysts generally used in the reforming processes (SR, DR, POX) can be also employed in the tri-reforming condition, noble metals (Pt, Rh, Ru) based catalysts show high performances and resistence to coke formation with respect to other transition metals as Nickel, however, the use of these elements increases the total cost of the catalytic materials [25]. Many studies have demonstrated that nickel can be used as active phase in catalysts for the tri-reforming process, if dispersed over supports that promote strong metal interaction as ceria, zirconia, titanium dioxide or mixed oxides as ceria–zirconia, ceria–lanthana, coupled with high O_2 storage features, all these properties contribute to reduce the carbon deposition and at the same time to increase the catalyst performances [26–28].

Despite the interest in a combined tri-reformer/SOFC process, limited efforts have been made in literature to study such systems [*inserire qualche riferimento bibliografico*]. The experimental set up and tests under different operative conditions were already approached for such combined process [1]. As a step forward, the main purpose of the present

work is the modeling and simulation of the combined process and the comparison of the numerical results with the available experimental data. In fact, the biogas-fed SOFC and trireforming system is quite cumbersome to characterize due to the unavailability of dedicated models in the existing process simulators (e.g., AspenHysys, UniSim, PRO/II). Only recently some basic models for fuel cells have been inserted in such systems, but they still lack in wide-range validation. Moreover, systems involving complex kinetics are still very challenging for process-scale simulations and industrial scale-up as well, due to complexities in formulating them but also in solving them efficiently and with appropriate reliability. This work tries to couple for the first time different tools for process simulations to provide a unified picture of the biogas-fed SOFC system.

2. Combined tri-reformer/SOFC process modeling

Fig. 1 depicts the combined process flow sheet: biogas (Stream 1) is fed to a heat exchanger (Biogas Heater) where it is heated to the temperature of the tri-reformer by the flue gas coming from the furnace (Stream 10). The stream is then fed to the tri-reformer where the dry reforming, steam reforming and partial oxidations reactions take place. The reformed biogas (Stream 5), henceforth called “reformed”, is sent to the anode of the fuel cell. Meanwhile, air (Stream 2) is sent to a heat exchanger (SOFC Air Heater) where it is heated to the fuel cell temperature (800 °C) by the flue gas from the furnace (Stream 10). The pre-heated air is then directed to the cathode of the fuel cell (Stream 6). In the solid oxide fuel cell the electrochemical reactions between the oxygen (present in air) and the hydrogen (present in the reformed) take place resulting in two exhausted streams. The first (Stream 7) is the exhausted reformed and is directed to the mixer, while the second (Stream 8) is the exhausted air channelled toward the heat exchanger (Furnace Air Heater) to pre-heat an additional air stream (Stream 3), which is then supplied to the mixer. Both the exhausted reformed (Stream 7) and the pre-heated air (Stream 9) are mixed in the same chamber (mixer) and then supplied to the furnace for the post-burning process. As already mentioned, the flue gas from the furnace (Stream 10) pre-heats the air and the biogas fed to the SOFC; then it produces steam in the boiler (Stream 4); steam which is then expanded in a turbine to produce electricity, before being supplied to the trireforming reactor.

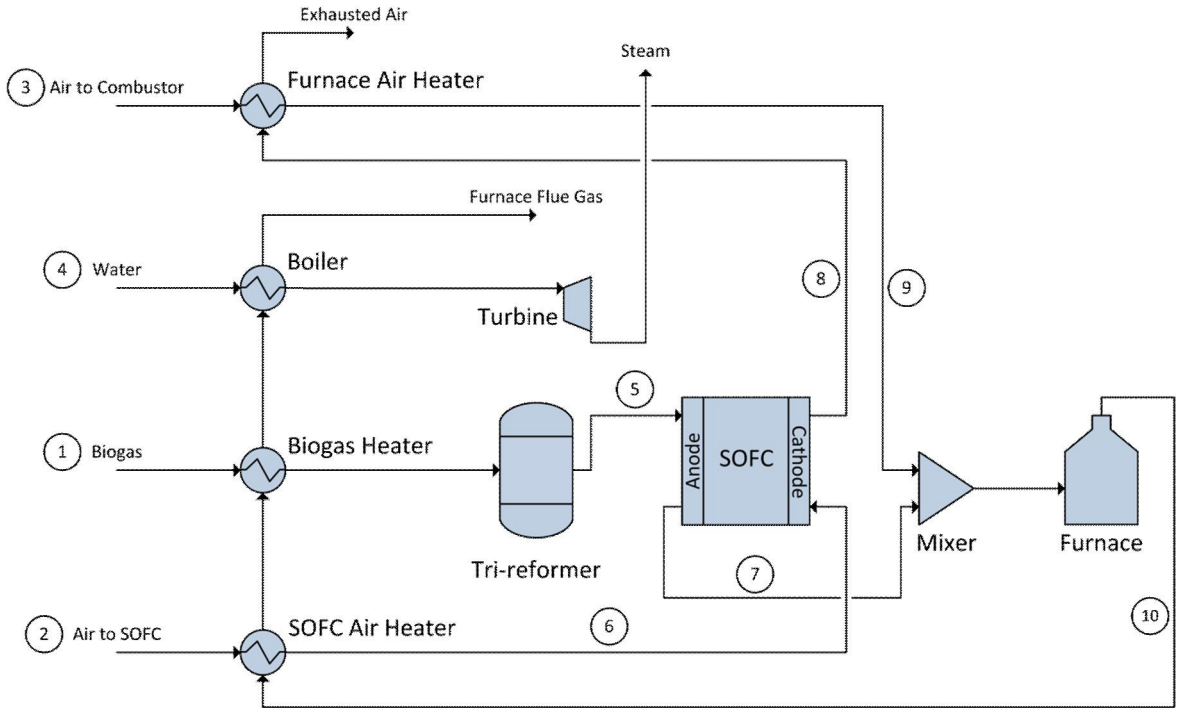

Fig. 1: Combined tri-reformer/SOFC process flowsheet.

The simulation of the process was performed using PRO/II® 8.3 software (Schneider Electric Simulation Science); SOFC and furnace operations were instead simulated using ad-hoc models linked to the main simulator, as it will be explained later.

2.1 Tri-reformer model

As stated earlier, the tri-reforming process consists of a combination of three catalytic processes in a single step: dry reforming (DR), steam reforming (SR) and partial oxidation (POX), whose reactions are specified below.

$$DR: \quad CH_4 + CO_2 \leftrightarrow 2CO + 2H_2 \qquad \Delta H_{298K} = 247.3\ \text{kJ/mol} \qquad (1)$$

$$SR: \quad CH_4 + H_2O \leftrightarrow CO + 3H_2 \qquad \Delta H_{298K} = 206.3\ \text{kJ/mol} \qquad (2)$$

$$POX: \quad CH_4 + \tfrac{1}{2}O_2 \leftrightarrow CO + 2H_2 \qquad \Delta H_{298K} = -35.6\ \text{kJ/mol} \qquad (3)$$

The biogas (CH_4=60% , CO_2=40%) tri-reforming process operates at thermodynamic equilibrium conditions, thus a Gibbs reactor is used in the simulation. This reactor solves the set of reactions and also the phase equilibria by minimizing the Gibbs free energy only assuming the mass balance [29]. The reactor temperature was set to 800 °C, the O_2/CH_4 and H_2O/CH_4 molar ratios were varied between 0.05-0.1 and 0.3-07 respectivelly as reported in table 1 and 2. The selected equation of state is the Soave-Redlich-Kwong (SRK) [30].

Moreover, the water gas shift reaction (WGS) and the total oxidation of methane (TOX) can also occur and have been taken into account in the tri-reforming model:

$$TOX: \quad CH_4 + 2O_2 \leftrightarrow CO_2 + 2H_2O \qquad \Delta H_{298K} = -880.0\ kJ/mol \tag{4}$$

$$WGS: \quad CO + H_2O \leftrightarrow CO_2 + H_2 \qquad \Delta H_{298K} = -41.09\ kJ/mol \tag{5}$$

As mentioned above, the main aspect of this work is the accomplishment of a model that takes in proper account the tri-reforming process and a solid oxide fuel cell (described in the next paragraph). In particular, the main assessment of such approach is that the composition of the stream from the reforming section, evaluated by using the PRO/II® software, represents the inlet gas fed to the SOFC's anode.

n.b.*: Il software del tri-reforming (anche se di tipo commerciale) è descritto troppo sinteticamente; inoltre, potrebbe essere utile inserire una figura (tipo la Fig. 4.1 della tesi di Vallevi), che attesti l'effettivo utilizzo di PRO/II.*

2.2 Solid oxide fuel cell model

The electrochemical reactions involved in a solid oxide fuel cell are the following.

$$Anode: \quad H_{2(g)} + O^{2-} \leftrightarrow H_2O_{(g)} + 2e^- \tag{6}$$

$$Cathode: \quad \frac{1}{2}O_{2(g)} + 2e^- \leftrightarrow O^{2-} \tag{7}$$

$$Global: \quad H_{2(g)} + \frac{1}{2}O_{2(g)} \leftrightarrow H_2O_{(g)} \tag{8}$$

An ad-hoc model was developed to simulate the electrochemical behaviour of a SOFC button cell; this modeling allows the calculation of parameters such as the current density, the cell voltage and the gas composition of the outlet stream from both anode and cathode of the fuel cell. The model consists of a non-linear system built up with the operative voltage of the cell $V_{OP}(i)$ as a function of the current density, as described in Eq. (9).

$$V_{OP}(i) = V_{REV} - \eta_{OHM} - \eta_{ACT} - \eta_{CONC} \tag{9}$$

where V_{REV} is the reversible potential, also called open circuit voltage (OCV), given by the well-known Nernst equation:

$$V_{REV} = -\frac{\Delta G_{TRN}}{2F} + \frac{R_g T}{2F} \ln\left(\frac{\left(\frac{P_{H_2}}{P_{Ref}}\right)\left(\frac{P_{O_2}}{P_{Ref}}\right)^{0.5}}{\left(\frac{P_{H_2O}}{P_{Ref}}\right)} \right) \tag{10}$$

The other terms of Eq. (9) are related to the losses inside the whole fuel cell represented by the ohmic losses (η_{OHM}), activation losses (η_{ACT}) and concentration losses (η_{CONC}).

Definitions of the remaining parameters may be found in the Nomenclature.

2.2.1 Ohmic losses

The ohmic losses are directly related to the resistance to the electron flow in the electrodes and the resistance to the ionic flow in the electrolyte. The associated potential loss is calculated as

$$\eta_{OHM} = i \cdot R \tag{11}$$

The value of the resistance R can be obtained theoretically, but for a rigorous determination it should be related to the operative conditions (e.g. temperature) and structure (thickness, materials, etc.) of each component of the cell, including both ionic and electronic mechanisms of conduction. Here, we preferred to use a value obtained experimentally from the impedance spectra of the simulated cell [1]: values in the order of 0.27-0.43 ohm cm^2 have been derived

2.2.2 Activation losses

Activation losses are related to the energy barrier that the reactive species must overcome in order to sustain the reaction. Activation polarization is usually described by the Butler-Volmer equation [31], [32]:

$$J = J_0 \left\{ \exp\left(\beta \frac{n_e F \eta_{ACT}}{R_g T} \right) - \exp\left(-(1-\beta) \left(\frac{n_e F \eta_{ACT}}{R_g T} \right) \right) \right\} \tag{12}$$

As suggested in literature [33], a good approximation of the Butler-Volmer equation, when the charge transfer reaction is assumed to be a one-step single electron transfer process, is the hyperbolic sine approximation: such an equation can be simplified for the case $\beta = 0.5$, to become [31]:

$$\eta_{ACT} = \frac{2R_g T}{n_e F} \sinh^{-1}\left(\frac{J}{2J_0} \right) \tag{13}$$

The exchange current density J_0 represents the equilibrium electron flow from cathode to anode and vice versa, and is calculated from the Arrhenius law [34]:

$$J_0^{Anode} = \gamma^{Anode} \left(\frac{P_{H_2}}{P_{Ref}} \right) \left(\frac{P_{H_2O}}{P_{Ref}} \right) \exp\left(-\frac{E_A^{Anode}}{R_g T} \right) \tag{14}$$

$$J_0^{Cathode} = \gamma^{Cathode} \left(\frac{P_{O_2}}{P_{Ref}} \right)^{0.25} \exp\left(-\frac{E_A^{Cathode}}{R_g T} \right) \tag{15}$$

at the anode and cathode, respectively.

The values of the pre-exponential coefficients γ and the activation energy E_A, at the anode and cathode, are specified in Table 1.

Table 1: *values of the pre-exponential coefficients and activation energies used in the model.*

Parameter		Value	Reference
E_a anode	[J mol^{-1}]	$1.34 \cdot 10^{10}$	[35]
E_a cathode	[J mol^{-1}]	$2.05 \cdot 10^{9}$	
γ anode	[A m^{-2}]	$1.05 \cdot 10^{4}$	
γ cathode	[A m^{-2}]	$1.1 \cdot 10^{5}$	

2.2.3 Concentration losses

Concentration losses are related to the mass transfer resistance of the reacting species within the pores of the electrodes. Reacting species have to diffuse through the pores of the electrodes to reach the sites where the electrochemical reaction takes place. Low gas concentration in the pores of the electrodes may limit the current and cause an increase of polarizations. In agreement with literature [36], the concentration polarization is calculated as follows:

$$\eta_{CONC} = \frac{R_g T}{n_e F} \ln\left(1 - \frac{J}{J_{lim}}\right) \quad (16)$$

The limiting current density J_{lim} is referred to as the maximum current density achieved in the case of complete reaction of the hydrogen present in the anode chamber. It depends both on molecular and Knudsen diffusion coefficients of the reactive species [31], and it is a function of the porosity, tortuosity and thickness of the electrode.

A rough estimation of J_{lim} can be obtained by the following equation

$$J_{lim} = \frac{F_{H_2}^{cell} n_e F}{A_{Active}} \quad (17)$$

n.b.: Questa equazione mi lascia molto perplesso, per quanto ne so, non ha alcun riscontro in letteratura (neanche nel citato Ref.[19]), e potrebbe essere fonte di critica da parte dei referee dell'articolo. Potrebbe essere meglio assumere un valore costante di corrente limite!?

2.3 Furnace model

A thermal furnace is used for the combustion of the outlet stream from the anodic chamber of the SOFC. The energy released in such combustion is then valorized for the pre-heating of the inlet streams (biogas, air to SOFC, and water). An ad-hoc model was adopted for the simulation of the furnace; for this purpose the DSMOKE software [37] has been used. The DSMOKE software, developed at the Polytechnic University of Milan, is a well-tested code [38, 39], which uses detailed kinetic scheme for the simulation of non-ideal chemical reactors, and can include more than 500 species and 30000 reactions. It is characterized by generality and modularity so as to allow the possibility to select a reduced number of chemical kinetics schemes according to the system to be modelled. Moreover, it allows to model series of ideal reactors in order to represent with higher accuracy and without any computational fluid dynamics study complex and non-ideal industrial systems thanks to appropriate combinations of ideal steps. In the specific case of the paper, the reactor selected for the simulation is a non-isothermal plug-flow reactor operating at atmospheric pressure with a volume

equal to $5 \times 10^{-4}\ m^3$, and the selected kinetic scheme includes only few families of reactions (hydrogen-oxygen, light hydrocarbons, oxidation), which allows to keep computational effort small.

As in acquaintance of the authors, the DSMOKE was never included in simulations at the process scale and its integration required the development of dedicated files and tools according to OPC (OLE for Process Control) directives. Microsoft Excel was adopted as hub for all the information of the different tools and models adopted (Figure XXX). PRO/II communicate with MS Excel thanks to ad hoc macros predisposed to exchange information with external simulation environments [40]. MS Visual C++ model for the SOFC and DSMOKE Suite communicate with MS Excel by means of I/O (Input/Output) ASCII files and special functions to read and write the exchanged information. Petri network techniques [41] are adopted to prevent any transmission problem.

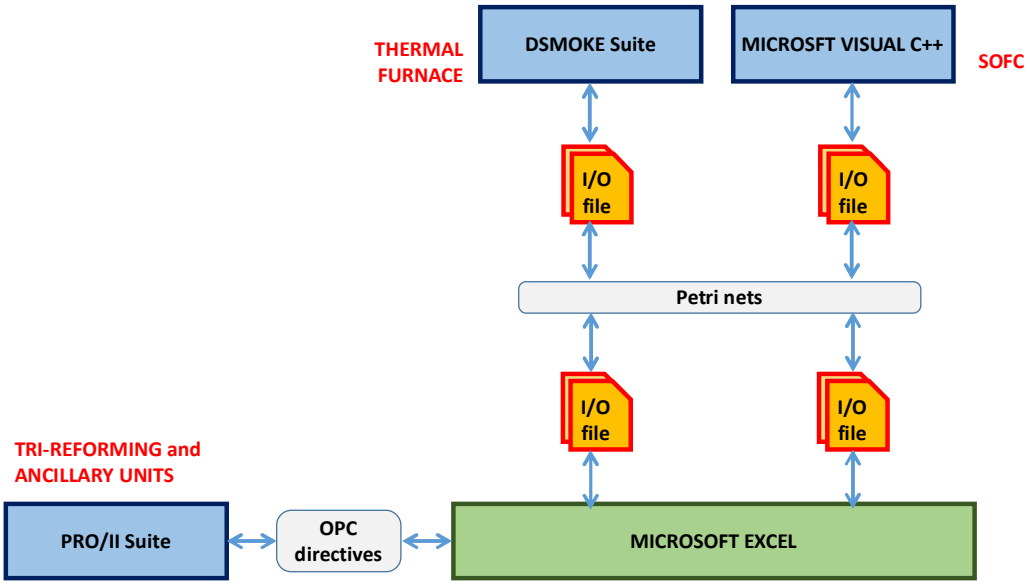

Fig. 2: Model integration via Microsoft Excel as information hub for process computing.

3. Results and model validation

The available experimental data at the selected operative condition [6] allowed to validate the models developed in the simulation of the system. In particular, the results obtained from the simulation of the tri-reforming model, the SOFC model, and the overall combined process model were compared. Such comparisons are described in the following sections.

3.1 Tri-reforming model

Four experimental tests, at different temperatures, were carried out in order to validate the tri-reforming model used in the simulation at a wide-range conditions. The selected temperatures were 795°C, 840°C, 900°C and 950°C. The assumption of isothermal operation and quasi-equilibrium conditions have been modelled using the so-called

temperature approach of PRO/II (with a the temperature in the order of 10 °C less than the experimental temperature), which is well-established in the process simulation of such systems.

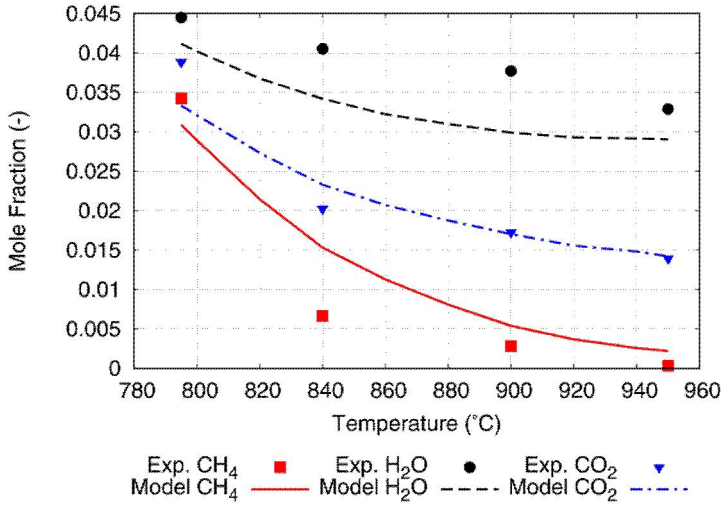

Fig. 3: CH_4, H_2O and CO_2 outlet molar composition for the tri-reforming process; experimental and model values.

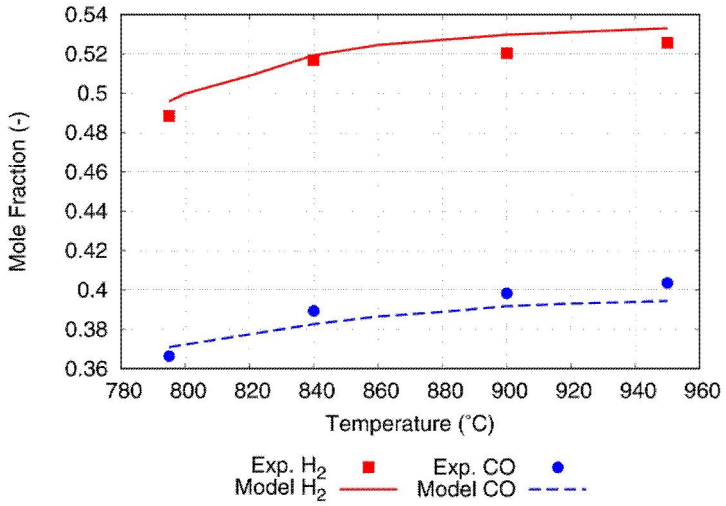

Fig. 4: H_2 and CO outlet molar composition for the tri-reforming process; experimental and model values.

In Fig. 3 and Fig. 4 the outlet molar composition obtained by the model (described in paragraph 2.1) and the experimental values, at the temperatures indicated, are shown. There is a good agreement between the model and the experimental data, with the exception of the water mole fraction that seems to be underestimated by the model. However, this may be due to a lacking during the experimental evaluation of low concentrations of water.

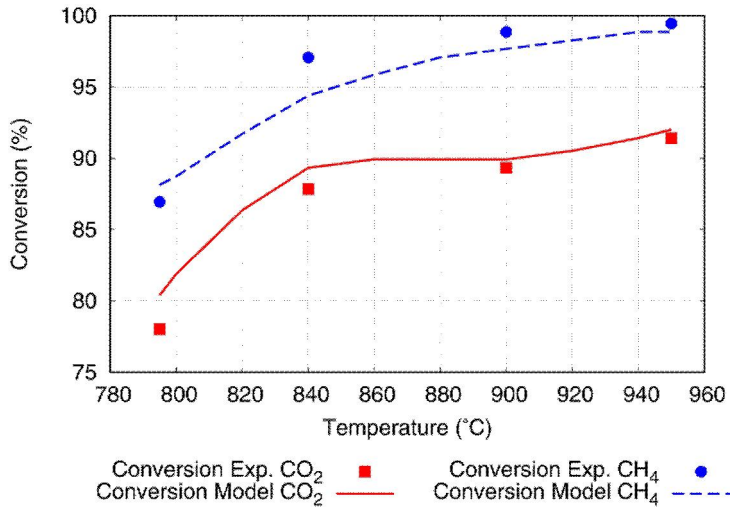

Fig. 5: Conversion profiles for CO_2 and CH_4: experimental and model values.

The conversion profiles for CO_2 and CH_4, from both experimental and model data, are shown in Fig. 5. As expected from the thermodynamic equilibrium, an increase in temperatures is beneficial for the two endothermic reactions (DR and SR) resulting in a higher conversion of CH_4 and CO_2. Subsequently, several tests (ranging from #1 to #9) with different inlet compositions were carried out at a fixed temperature (800 °C). Table shows the CO and H_2 outlet composition obtained by experimental tests and by calculation; for each test, the difference between these values was less than 4%.

Table 2: Outlet composition of the tri-reforming process with different inlet molar ratio.

Test	Inlet molar ratio			Model outlet composition [mole]		Exp. outlet composition [mole]	
	CH_4/CO_2	O_2/CH_4	H_2O/CH_4	CO	H_2	CO	H_2
#1	1.5	0.10	0.7	0.320	0.522	0.328	0.519
#2	1.5	0.08	0.7	0.324	0.527	0.333	0.522
#3	1.5	0.05	0.7	0.328	0.534	0.337	0.532
#4	1.5	0.10	0.5	0.351	0.527	0.356	0.523
#5	1.5	0.08	0.5	0.354	0.531	0.362	0.529
#6	1.5	0.05	0.5	0.359	0.537	0.372	0.532
#7	1.5	0.10	0.3	0.384	0.525	0.394	0.532
#8	1.5	0.08	0.3	0.387	0.528	0.394	0.531
#9	1.5	0.05	0.3	0.390	0.530	0.398	0.543

Complete data regarding the conversion of methane and carbon dioxide are shown in Table . Also in this case the the experimental and the model values are in very good agreement for each test with differences lower than 4%. Therefore, the Gibbs reactor is able to predict with a proper reliability the tri-reforming process, demonstrating that it operates at thermodynamic equilibrium.

Table 3: CH_4 and CO_2 conversion for the tri-reforming process with different inlet molar ratio.

Test	Inlet molar ratio			Model conversion [%]		Exp. Conversion [%]	
	CH_4/CO_2	O_2/CH_4	H_2O/CH_4	CH_4	CO_2	CH_4	CO_2
#1	1.5	0.10	0.7	98.4	65.5	99.4	67.6

#2	1.5	0.08	0.7	98.2	67.7	99.4	70.1
#3	1.5	0.05	0.7	97.9	70.1	99.4	74.3
#4	1.5	0.10	0.5	97.6	76.2	99.2	78.3
#5	1.5	0.08	0.5	97.3	78.4	99.2	80.5
#6	1.5	0.05	0.5	96.7	81.5	99.1	84.2
#7	1.5	0.10	0.3	95.8	86.7	99.0	88.9
#8	1.5	0.08	0.3	95.1	88.6	97.6	90.2
#9	1.5	0.05	0.3	93.7	90.8	96.0	93.9

3.2 SOFC model

The fuel cell model has been validated by using the available experimental data. A comparison between the experimental and calculated polarization curves, for each of the considered tests, was assessed.

Inserire una tabella con tutti i dati di input del modello.

Table 4: Input data for the SOFC model

Parameter	Value	Reference
E_a anode [J mol^{-1}]	$1.34 \cdot 10^{10}$	[35]
E_a cathode [J mol^{-1}]	$2.05 \cdot 10^{9}$	[35]
γ anode [A m^{-2}]	$1.05 \cdot 10^{4}$	[35]
γ cathode [A m^{-2}]	$1.10 \cdot 10^{5}$	[35]
β [-]	0.5	-
F [C mol^{-1}]	96485	-
R [J K^{-1} mol^{-1}]	8.314	-
T [K]	1073	-
P [bar]	1.013	-

The polarization curves for tests #1, #2 and #3 (see Table 1, for test specifications) are shown in Fig. 6. It can be seen that the model profile agrees quite well with the experimental data in the middle region of the curves. The most significant difference occurs in proximity of the open circuit voltage (OCV), and it is mainly due to the simplifications introduced by the Butler-Volmer equation. Nonetheless, such a deviation is within a region where conventionally the fuel cell does not operate. Analogous results are observed in Fig. 7 and Fig. 8.

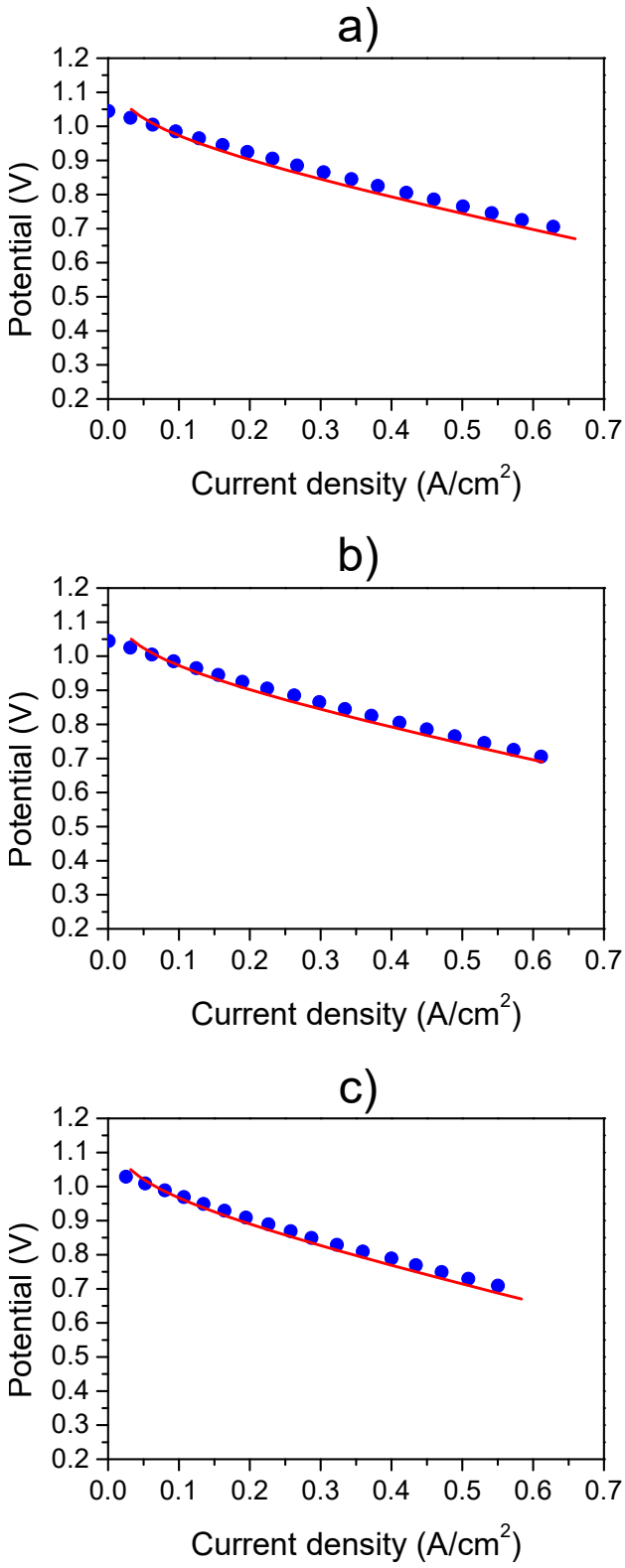

Fig. 6: Polarization curves for a) Test #1; b) Test #2 and c) Test #3. Symbols (●) represents experimental data. Solid line (—) represents model data.

Another offset between the data (see Fig. 7, in particular) is that the modeled curves are slightly lower than the experimental data in the region dominated by the ohmic polarization. This behaviour arises from difficulties in evaluating the exact ohmic losses within the cell. Particularly evident is the deviation between data in the case of a lower methane

conversion in the tri-reforming process (see Fig. 8 c). In this case a fast deactivation of the Ni-based anode may be predicted, due to the formation of carbonaceous deposits inside the pores of the cell that can lead to its partial or total occlusion [1]; Therefore, a decrease of the cell efficiency in the experimental curves and an overestimation of the cell voltage by the model is reasonable.

1) *Per quale ragione solo nel caso delle Figure 6a,b,c si osserva una "inability to proper quantify the ohmic losses", e negli altri casi no?*
2) *In realtà praticamente nel modello venivano sottostimate le perdite per concentrazione, quindi anche la discrepanza nella parte centrale dipendeva dalla mancanza di queste.*
3) *Non si nota, né nelle curve sperimentali, né in quelle calcolate, la caduta dovuta alle perdite diffusionali, tipica delle alte densità di corrente (per la verità, nelle curve sperimentali non si osserva nemmeno la caduta dovuta alle perdite di attivazione). Come mai? Per il modello, vedere sopra.*

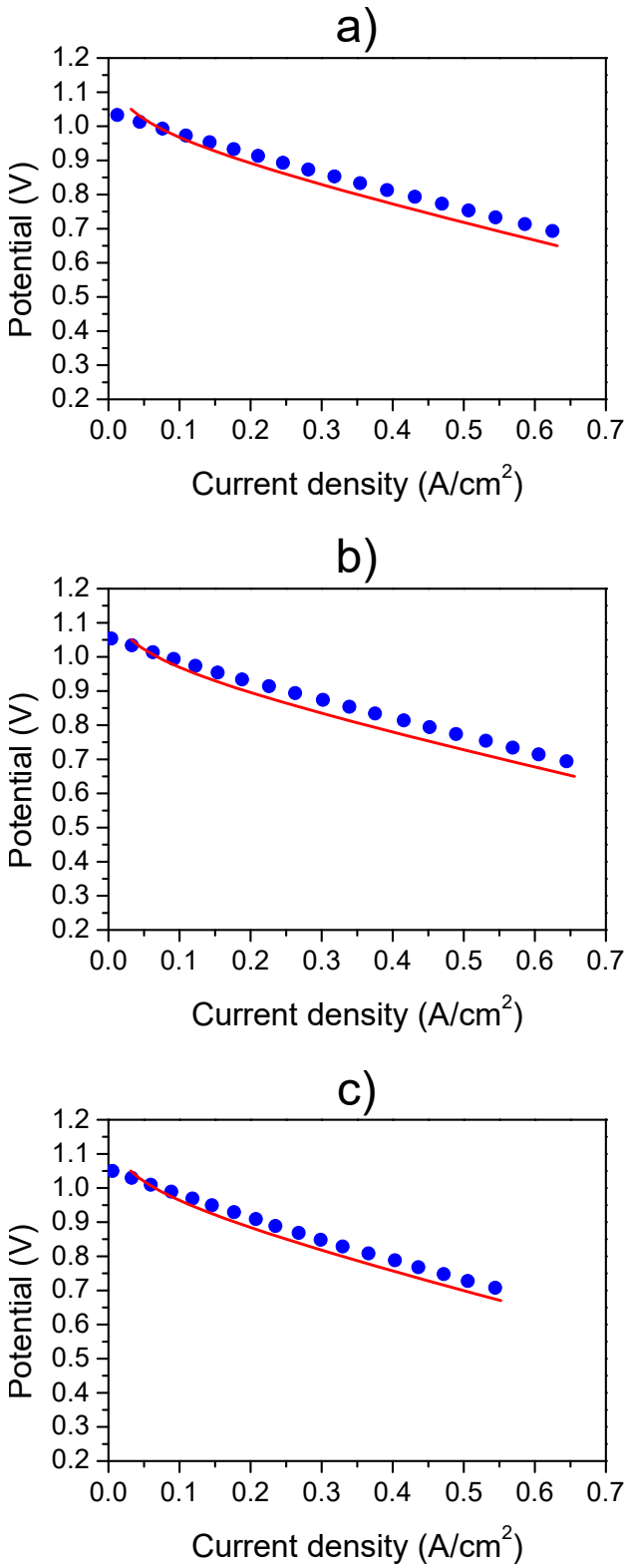

Fig. 7: Polarization curves for a) Test #4; b) Test #5 and c) Test #6. Symbols (●) represents experimental data. Solid line (—) represents model data.

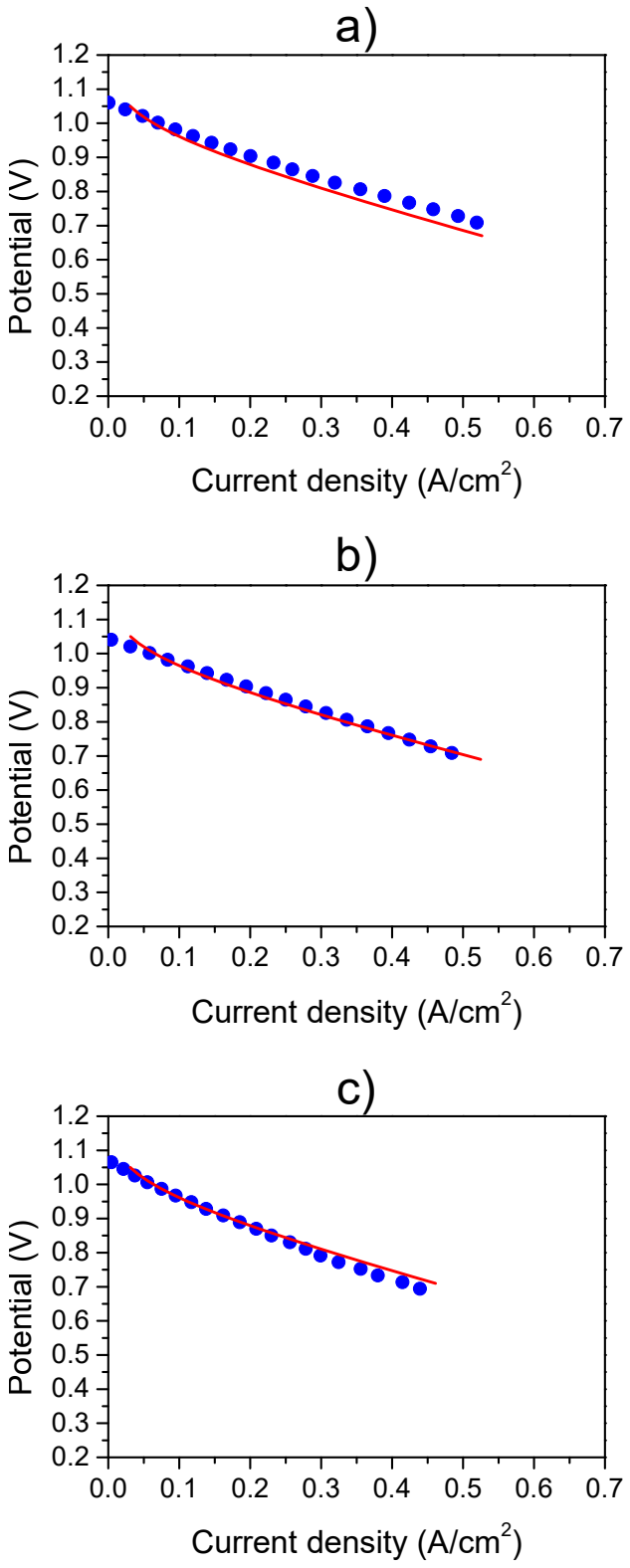

Fig. 8: Polarization curves for a) Test #7; b) Test #8 and c) Test #9. Symbols (•) represents experimental data. Solid line (—) represents model data.

4. Process-scale performance

Once the model was validated, the overall system (described in paragraph 2) was assessed and simulated with the conditions equal to those developed during the experimental tests, i.e. biogas flow into the tri-reforming reactor at a rate of $100\,cm^3/min$ and SOFC potential fixed to 0.8 V. Table 1 shows the current density error between the model and the experimental data. For each test the error was below the 10%, that may be considered reasonable since it is of the same order of the experimental error.

Table 1: Comparison of current density obtained by model and experimental values (@ 0.8 V).

Test	Exp. current density $[A/cm^2]$	Model current density $[A/cm^2]$	Error [%]
#1	0.42	0.41	3.65
#2	0.41	0.41	0.45
#3	0.36	0.37	2.00
#4	0.43	0.40	8.27
#5	0.45	0.41	9.63
#6	0.37	0.36	2.45
#7	0.35	0.33	5.63
#8	0.34	0.36	6.78
#9	0.30	0.31	2.98

It is noteworthy that the current density, and hence the cell performance, decreases with the gradual decrease of CH_4 conversion; thus, supporting the fact that the formation of carbon deposits may depress the charge transfer process by poisoning the sites inside the porous electrode.

The utilization factor (u) of a fuel cell is defined as the ratio between the fuel consumed and the fuel provided to the cell.

$$u = \frac{F_{H_2,i}^{cell} - F_{H_2,o}^{cell}}{F_{H_2,i}^{cell}} \tag{18}$$

The utilization factor has a big influence on the cell efficiency; in fact, according to Wen et al. [42], when dealing with the optimization of solid oxide fuel cells the utilization factor is a key parameter, together with the cell configuration.

Table 2: Cell utilization factor and hydrogen inlet and outlet composition.

Test	u [%]	Inlet H_2 composition [mole]	Outlet H_2 composition [mole]
#1	6.82	0.52	0.49
#2	6.76	0.53	0.49
#3	6.02	0.53	0.50
#4	6.06	0.53	0.49
#5	6.01	0.53	0.50
#6	4.96	0.54	0.51
#7	5.29	0.53	0.50
#8	5.59	0.53	0.50
#9	5.26	0.53	0.50

Low values of utilization factor (in the range of about 5-7%) were obtained, as shown in Table 2. These values were expected to be due to the size of the system: in fact, the fuel provided to the cell is almost ten times those predictable from the Faraday's equation. Additionally, the slight variation of the utilization factor – in each of the tests – cannot be

attributed to the variation of the hydrogen concentration, that is almost constant (see Table 4) in all tests. Thus, the change in the ohmic losses is responsible of the reduction of the utilization factor; indeed, increasing ohmic losses causes a decrease in current density, and therefore reduces the amount of hydrogen converted into the cell. As a result, the efficiency of the fuel cell is very low ($\sim 2.5\ \%$) and, despite the introduction of heat recovery units and other power generation systems (such as the turbine) downstream, the overall performance of the system is also very low (efficiency $\sim 4\ \%$).

Although it is out of the scope of the present study to model a real system, due to the characteristic and size of the equipment used for the experimental tests; nevertheless, the presented model could be easily applied to larger systems with only minimal modifications. Moreover, it could be helpful in studying system feasibility and optimization assessment, in order to increase the overall system performance.

n.b.: Non si capisce dove, e come, entra in gioco il modello del combustore (furnace model); inserire qualche frase esplicativa al riguardo e, possibilmente, qualche risultato legato al combustore.

Potrebbe essere il caso di inserire le equazioni per il calcolo delle efficienze.

5. Conclusions

The necessity to explore alternative energy sources not dependent on fossil fuels, the rising concern in environmental issues altogether with the usual interest in economic growth have encouraged the investigation of new technologies based on renewable fuels. One way to tackle such issues is through the use of biofuels, such as biomass or biogas, and the integration of chemical processes to decrease emissions while increasing energy efficiency and profitability of the process. Thus, we have presented a first development of a model of an integrated tri-reformer/SOFC system based on biogas for the production of sustainable and clean energy. Such a process appears to be a promising approach to contribute in the reduction of carbon footprint, in comparison with the usual power generation system based on the combustion of fossil fuels. The proposed model, validated with experimental data, has the ability to reproduce a micro-scale plant quite accurately under a variety of conditions, resulting in a flexible solution capable of being scaled-up to the study of larger systems.

n.b.: Nelle conclusioni andrebbe inserito qualche commento sui risultati ottenuti da/dail modello/modelli, con considerazioni sia in termini quantitativi che qualitativi.

Nomenclature

A_{active}	active area of the fuel cell	$[m^2]$
E_A	activation energy for reaction in electrode	$[J/mol]$
F	Faraday constant	$[A \cdot s/mol]$
$F_{i,i}^{cell}$	inlet molar flow of species i to the fuel cell	$[mol/s]$
$F_{i,0}^{cell}$	outlet molar flow of species i to the fuel cell	$[mol/s]$
ΔG_{rxn}	change of reaction's Gibbs free energy	$[J/mol]$

j	current density	$[A/m^2]$
j_o	exchange current density	$[A/m^2]$
j_{lim}	limiting current density	$[A/m^2]$
n_e	number of reacting electrons	[–]
P_i	partial pressure of species i	[Pa]
P_{Ref}	reference pressure	[Pa]
R_g	universal gas constant	$[J/mol \cdot K]$
T	temperature	[K]
η_{ACT}	activation polarization	[V]
η_{CONC}	concentration polarization	[V]
η_{OHM}	ohmic polarization	[V]
V_{OP}	operative voltage	[V]
V_{REV}	reversible potential of the cell (OCV)	[V]

Greek letters

β	transfer coefficient	[–]
γ	pre-exponential factor for reaction in electrode	$[A/m^2]$

References

Sarebbe bene aggiungere qualche altro riferimento bibliografico, stando attenti a riordinare la numerazione nel testo.

[1] Lo Faro M, Vita A, Pino L, Aricò AS. Performance evaluation of a solid oxide fuel cell coupled to an external biogas tri-reforming process. Fuel Processing Technology. 2013;115:238-45.

[2] Ediger VŞ, Hoşgör E, Sürmeli AN, Tatlıdil H. Fossil fuel sustainability index: An application of resource management. Energy Policy. 2007;35:2969-77.

[3] Dunn S. Hydrogen futures: toward a sustainable energy system. International Journal of Hydrogen Energy. 2002;27:235-64.

[4] Ball M, Wietschel M. The future of hydrogen – opportunities and challenges. International Journal of Hydrogen Energy. 2009;34:615-27.

[5] Winter C-J. Hydrogen energy — Abundant, efficient, clean: A debate over the energy-system-of-change. International Journal of Hydrogen Energy. 2009;34:S1-S52.

[6] Effendi A, Zhang ZG, Hellgardt K, Honda K, Yoshida T. Steam reforming of a clean model biogas over Ni/Al2O3 in fluidized- and fixed-bed reactors. Catal Today. 2002;77:181-9.

[7] W. Edelmann. Biogas production and usage. In: Kaltschmitt M, Hartmann H, editors. Energy from biomass: basic principles, technologies and processes. Leipzig, Germany: Springer; 2001.

[8] Van herle J, Membrez Y, Bucheli O. Biogas as a fuel source for SOFC co-generators. Journal of Power Sources. 2004;127:300-12.

[9] Xuan J, Leung MKH, Leung DYC, Ni M. A review of biomass-derived fuel processors for fuel cell systems. Renewable and Sustainable Energy Reviews. 2009;13:1301-13.

[10] Larminie J, Dicks A. Fuel Cell Systems Explained. 2nd ed. Chichester, UK: John Wiley & Sons; 2003.

[11] EG&G Technical Services Inc. Fuel Cell Handbook. 7th ed: U.S. Department of Energy; 2004.

[12] Papadias DD, Ahmed S, Kumar R. Fuel quality issues with biogas energy – An economic analysis for a stationary fuel cell system. Energy. 2012;44:257-77.

[13] A. D. Ballarini, S. R. De Miguel, E. L. Jablonski, O. A. Scelza, A. A. Castro, Reforming of CH4 with CO2 on Pt-supported catalysts: effect of the support on the catalytic behaviour, Catal Today, 2005;107:481-486.

[14] F. Joensen, J. R. Rostrup-Nielsen, Conversion of hydrocarbons and alcohols for fuel cells, J. Power Sources 2002, 105:195-201.

[15] M. Benito, S. Garcıa, P. Ferreira-Aparicio, L. G. Serrano, L. Daza, Biogas reforming on La-promoted NiMgAl catalysts derived from hydrotalcite-like precursors, J Power Sources, 2007;169:177-183.

[16] P. Piroonlerkgul, S. Assabumrungrat, N. Laosiripojana, A. A. Adesina, Selection of appropriate fuel processor for biogas-fuelled SOFC system, Chem. Eng. J. 2008;140:341-351.

[17] S, Specchia, G Negro, G. Saracco, V. Specchia, Fuel processor based on syngas production via short-contact-time catalyticpartial- oxidation reactors. Appl Catal B e Environ 2007;70:525-31.

[18] C.S. Lau, A. Tsolakis, M.L. Wyszynski, Biogas upgrade to syn-gas (H2eCO) via dry and oxidative reforming, International Journal of Hydrogen Energy, 2011;36:397-404.

[19] P. Lidia , A. Vita, M. Cordaro, V. Recupero, M. S. Hegde, A comparative study of Pt/CeO2 catalysts for catalytic partial oxidation of methane to syngas for application in fuel cell electric vehicles, Applied Catalysis A: General;2003;31:135-146.

[20] B.C. Enger, R. Lødeng, A Holmen. A review of catalytic partial oxidation of methane to synthesis gas with emphasis on reaction mechanisms over transition metal catalysts. Appl Catal A General 2008;3461-27.21] Song C, Pan W. Tri-reforming of methane: a novel concept for catalytic production of industrially useful synthesis gas with desired H2/CO ratios. Catalysis Today. 2004;98:463-84.

[22] Izquierdo U, Barrio VL, Requies J, Cambra JF, Güemez MB, Arias PL. Tri-reforming: A new biogas process for synthesis gas and hydrogen production. Int J Hydrogen Energy. 2013;38:7623-31.

[23] Manenti F, Leon-Garzon AR, Ravaghi-Ardebili Z, Pirola C. Systematic staging design applied to the fixed-bed reactor series for methanol and one-step methanol/dimethyl ether synthesis. Appl Therm Eng. 2014;70:1228-37.

[24] Pirola C, Scavini M, Galli F, Vitali S, Comazzi A, Manenti F, et al. Fischer-Tropsch synthesis: EXAFS study of Ru and Pt bimetallic Co based catalysts. Fuel. 2014;132:62-70.

[25] M. Nawfal, C. Gennequin, M. Labaki, B. Nsouli, A. Aboukaïs, E. Abi-Aad, Hydrogen production by methane steam reforming over Ru supported on Ni–Mg–Al mixed oxides prepared via hydrotalcite routeOriginal Research Article, International Journal of Hydrogen Energy, 2015;40:1269-1277

[25] A. Vita, L. Pino, F. Cipitì, M. Laganà, V. Recupero, Biogas as renewable rawmaterial for syngas production by tri-reforming process over NiCeO2 catalysts: Optimal operative condition and effect of nickel content, Fuel Processing Technology, 2014; 127: 47-58

[26] L. Pino, A. Vita, M. Laganà, V. Recupero, Hydrogen from biogas: Catalytic tri-reforming process with Ni/LaCe O mixed oxides. Applied Catalysis B, Enviromental, 2014; 148-149: 91-105

[27] K. Tomishige, Y. G. Chen, K. Kujimoto, Studies on carbon deposition in CO2 reforming of CH4 over nickel–magnesia solid solution catalysts, J. Catal.1999; 181: 91-103.

[28] V. A. Tsipouriari, X. Verykios, Carbon and oxygen reaction pathways of CO2 reforming of methane over Ni/La2O3 and Ni/Al2O3 catalysts studied by isotopic tracing techniques, J. Catal. 187 (1999) 85-94.

[29] Towler G, Sinnott RK. Chemical Engineering Design: Principles, Practice and Economics of Plant and Process Design: Elsevier Science; 2007.

[30] Soave G. Equilibrium Constants from a Modified Redlich-Kwong. Equation of State. Chem Eng Sci. 1972;27:1197-203.

[31] Chan SH, Khor KA, Xia ZT. A complete polarization model of a solid oxide fuel cell and its sensitivity to the change of cell component thickness. Journal of Power Sources. 2001;93:130-40.

[32] Zhu H, Kee RJ, Janardhanan VM, Deutschmann O, Goodwin DG. Modeling Elementary Heterogeneous Chemistry and Electrochemistry in Solid-Oxide Fuel Cells. Journal of The Electrochemical Society. 2005;152:A2427-A40.

[33] Noren DA, Hoffman MA. Clarifying the Butler–Volmer equation and related approximations for calculating activation losses in solid oxide fuel cell models. Journal of Power Sources. 2005;152:175-81.

[34] Calise F, Vanoli L, Dentice d'Accadia M, Palombo A. One-Dimensional Model of a Tubular Solid Oxide Fuel Cell. Journal of Fuel Cell Science and Technology. 2008;5:021014-.

[35] Suther T, Fung A, Koksal M, Zabihian F. Macro Level Modeling of a Tubular Solid Oxide Fuel Cell. Sustainability. 2010;2:3549-60.

[36] Gebregergis A, Pillay P. The Development of Solid Oxide Fuel Cell (SOFC) Emulator. Power Electronics Specialists Conference, 2007 PESC 2007 IEEE2007. p. 1232-8.

[37] Manca D, Buzzi-ferraris G, Faravelli T, Ranzi E. Numerical problems in the solution of oxidation and combustion models. Combustion Theory and Modelling. 2001;5:185-99.

[38] Ranzi E, Corbetta M, Manenti F, Pierucci S. Kinetic modeling of the thermal degradation and combustion of biomass. Chem Eng Sci. 2014;110:2-12.

[39] Manenti F, Papasidero D, Bozzano G, Ranzi E. Model-based optimization of sulfur recovery units. Comput Chem Eng. 2014;66:244-51.

[40] Manenti F, Signor S, Grottoli MG, Fabbri P. Adaptive data reconciliation coupling C++ and PRO/II and on-line application by the field. Computer Aided Chemical Engineering2010. p. 373-8.

[41] Reisig W. Petri Nets and Algebraic Specifications. Theoretical Computer Science. 1991;80:1-34.

[42] Wen H, Ordonez JC, Vargas JVC. Optimization of single SOFC structural design for maximum power. Applied Thermal Engineering. 2013;50:12-25.